L-shell resonant transfer excitation in $Cu^{q+} + H_2$ ($q = 18,19$) collisions

P. A. Závodszky,* J. A. Wroblewski, S. M. Ferguson, T. W. Gorczyca, J. H. Houck, O. Woitke,† and J. A. Tanis
Department of Physics, Western Michigan University, Kalamazoo, Michigan 49008

N. R. Badnell
Department of Physics and Applied Physics, University of Strathclyde, Glasgow G4 ONG, United Kingdom
(Received 21 February 1997)

Resonant transfer excitation (RTE) involving $L^{-1}Mn$ ($n \geqslant M$) resonant states has been investigated for Na-like and Ne-like $Cu^{q+} + H_2$ collisions ($q = 18$ and 19). The M- to L-shell x-ray production cross sections (RTEX's) of these resonance states are studied by x-ray projectile ion coincidences. Previous measurements of L-shell RTEX for Nb^{q+} ($q = 28-31$) ions showed the measured cross sections to be nearly a factor of 2 smaller than the calculated ones. For Cu^{18+} the present results show the position and width of the measured RTEX maximum cross section to be in agreement with the calculations; however, the measured absolute cross sections are about 60% higher than the predicted ones. In the case of Ne-like Cu^{19+} projectiles, the metastable component in the beam made it impossible to observe RTEX's. [S1050-2947(97)07309-5]

PACS number(s): 34.70.+e

I. INTRODUCTION

In atomic collision involving ions and atoms there are three important categories of processes: excitation, ionization, and charge transfer. In many situations one can describe the phenomena which occur only by taking into account the Coulomb interaction between the participating nuclei and the electrons. However, there are some notable exceptions, where one cannot neglect the interaction between electrons, and, indeed, sometimes this interaction is dominant. In the past decade there has been much interest, both theoretically and experimentally, to examine processes where the electron-electron interaction is important. According to McGuire [1], there are two types of electron correlation: static and dynamic. The former case has to be taken into account in atomic structure calculations, and the latter one may have an important role during certain collision processes.

A striking example of a process where the electron-electron interaction has an important role in ion-atom collisions is the process called resonant transfer excitation (RTE), first uncovered in the early 1980s [2,3]. In this process an electron from the target and another from the projectile interact so that the target electron is captured to the projectile with a simultaneous projectile excitation, giving rise to a doubly excited intermediate state. This state will subsequently decay either by the emission of Auger electrons or photons. This charge transfer and excitation occurs in a manner completely analogous to dielectronic recombination (DR) [4], which occurs in electron-ion collisions. In DR, formation of the intermediate excited state proceeds via the inverse of an Auger transition, and is resonant for relative velocities corresponding to ejected electron energies in the Auger process [5]. The analogy between DR and RTE was first formulated theoretically by Brant [6], who developed a unified treatment of these two processes using the impulse approximation. In RTE, the target electron can be considered quasifree if the projectile velocity is much larger than the target electron velocity. However, these quasifree electrons are no longer monoenergetic as in the case of DR, but have a characteristic momentum distribution, the so-called Compton profile. In the framework of the impulse approximation it is assumed that during a fast collision the momentum wave function of the target electron is undisturbed.

RTE was investigated by several groups either by measuring the x-ray production cross sections in coincidence with electron capture RTEX, or by measuring state-selective Auger electron emission as a function of projectile energy (RTEA). For a recent extensive review of RTEX, see Tanis [7]; for RTEA, see Zouros [8]. RTE has been studied for nearly the entire range of projectile atomic numbers, from He ($Z = 2$) to U (Z-92). The most suitable targets for these studies are those with relatively narrow Compton profiles, specifically H_2 and He.

The overwhelming majority of the RTE data and calculations to date is for K-shell excitation [7,8]. In general, the existing K-shell RTEX experimental cross sections are in reasonably good agreement with calculated RTEX cross sections based on theoretical dielectronic recombination cross sections convoluted with the experimentally determined [9] or theoretically calculated [10] Compton profiles of the target electrons. The results indicate that RTE is well understood within the framework of the impulse approximation utilizing the Auger and x-ray rates of doubly excited states that determine the DR cross sections.

There are only a few studies to date for RTE involving excitation of the projectile L shell [7]. In measurements by Bernstein and co-workers [11,12] for different charge states of $_{41}Nb^{q+}$ ($q = 28-32$), the measured RTEX cross sections were found to increase significantly with increasing charge state. Theoretical calculations [13,14] overestimated significantly these RTEX cross sections, contrary to the good agreement previously found between theory and experiment

*Present address: Kansas State University, Manhattan, KS 66506.
†Present address: Oak Ridge National Laboratory, Oak Ridge, TN 37831.

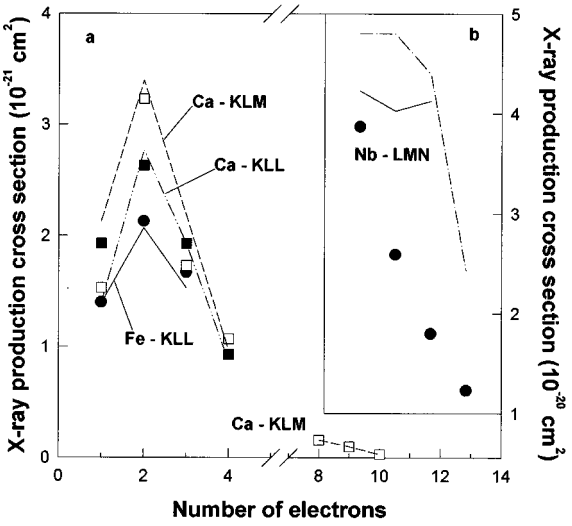

FIG. 1. Charge-state dependence of RTEX cross-section maxima. See Ref. [7] for citations to original data. (a) *K* shell. (b) *L* shell.

for *K*-shell RTEX. A comparison between theory and experiment for *K*- and *L*-shell RTEX cross sections is presented in Fig. 1, which is taken from Ref. [7]. Furthermore, in a recent DR experiment by Linkemann *et al.* [15] using Na-like Fe^{15+} ions, the theory overestimated the experiment by roughly a factor of 2. However, a more recent improved calculation has removed some of the discrepancy [16].

To further address this discrepancy between experiment and theory for *L*-shell RTE (or DR) cross sections, we began a systematic investigation of *L*-shell RTEX using different charge states of copper ions. A schematic of the RTE process for a Na-like Cu^{18+} ion is presented in Fig. 2. In Sec. II we present briefly the improved method of calculating *L*-shell RTE cross sections, in Sec. III we describe the experimental methods used, in Sec. IV we present the results obtained and the interpretation of the results, and in Sec. V we present a short summary and conclusion. A detailed discussion of the theoretical calculations is presented elsewhere [16].

II. THEORY

For high projectile energies where the impulse approximation [6] is valid, the RTEX cross section $\sigma_{\mathrm{RTE}}(E_p)$ for ions incident on atoms or molecules is related to the DR cross section, $\sigma_{\mathrm{DR}}(E_e)$, for electors incident on the same ion:

$$\sigma_{\mathrm{RTEX}}(E_p)=\int dp_z J(p_z)\sigma_{\mathrm{DR}}(E_e), \tag{1}$$

where the distribution of the target-electron momentum p_z is given by the Compton profile

$$J(p_z)=\int\int dp_z dp_y |\Psi(p_x,p_y,p_z)|^2, \tag{2}$$

and the electron energy is related to that momentum by

$$E_e=\frac{m}{M}E_p-E_t+p_z\sqrt{2E_p/M}, \tag{3}$$

where m and M are the electron and projectile masses, respectively, and E_t is the ionization threshold of the target atom or molecule.

Most calculations of $\sigma_{\mathrm{DR}}(E_e)$ make use of perturbative methods, involving independent processes and the isolated-resonance approximation. These results compare favorably with experimental measurements when *K*-shell excitation is involved [4,7,8], but overestimate the experiments roughly by a factor of 2 when *L*-shell RTEX [11,12] or DR [15] is involved.

In an earlier calculation by Badnell [14], *LS* coupling was used for Na-like $_{41}Nb^{30+}$ and only the $2p^5 3s 3lnl'$ configurations were included in the basis describing the resonance states. The other configuration involving a $2p$ hole and two *M*-shell electrons, i.e., $2p^5 3p^2 nl$, $2p^5 3p 3dnl$, and $2p^5 3d^2 nl$, were not included in this basis.

A new set of calculations using intermediate coupling was performed which includes configuration interaction (CI) between the directly accessible $2p^5 3s 3lnl'$ configuration and the other configurations mentioned above. All calculation used the program AUTOSTRUCTURE [17]. The RTEX cross sections were obtained from the DR cross sections by averaging them over the Compton profile [9] of H_2, taking into account the binding energy of the target electrons. Details and results which demonstrate the effects of configuration interaction and intermediate coupling are presented in a separate paper [16]. It is noted that the inclusion of the additional configurations brings theory more in line with experiment. This is apparently due to the fact that CI, combined with configuration which cannot radiatively decay to bound states, tends to redirect DR probability to other decay channels.

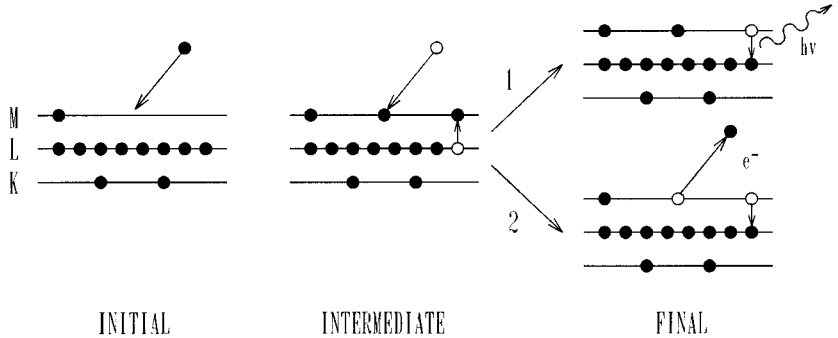

FIG. 2. Schematic of the RTE process for a Na-like Cu^{18+} ion. The intermediate doubly excited state is formed via electron capture accompanied by projectile excitation. This intermediate excited state subsequently decays either by photon emission (1) or by electron emission (2).

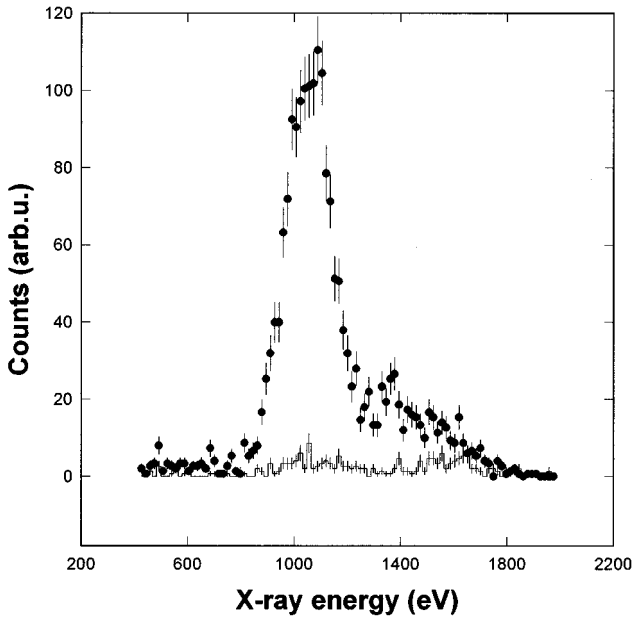

FIG. 3. Cu L x-ray spectrum as a function of x-ray energy for 65-MeV $Cu^{18+}+H_2$ collisions. ●, 50 m Torr H_2; —, background (no target gas).

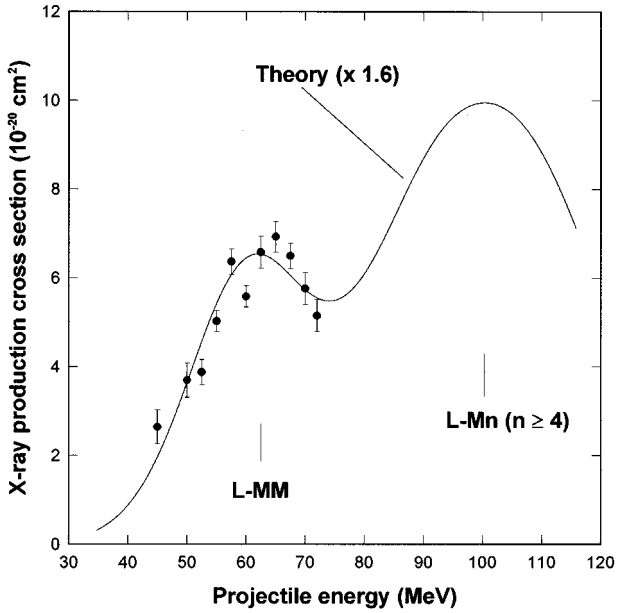

FIG. 4. X-ray production cross sections for single-electron capture coincident with L x-ray emission as a function of projectile energy in $Cu^{18+}+H_2$ collisions. The solid points are the present experimental data and the smooth curve shows the corresponding calculated RTEX cross sections multiplied by 1.6.

III. EXPERIMENTAL METHODS

The experiment was performed at Western Michigan University using the 6-MV tandem Van de Graaff accelerator. Cu^- ions were produced in a cesium sputter-ion source, and accelerated to the desired energy. Stripping at the terminal of the accelerator was accomplished with a carbon foil. Depending on the projectile energy a 90° analyzing magnet selected the $q=9$, 10, or 11 charge state and the isotope with atomic mass 65 emerging from the accelerator. This ion was subsequently post-stripped in a second carbon foil, and the desired charge state ($q=18$ or 19) was magnetically selected with a 30° switching magnet and directed toward the experimental apparatus. After collimation the ion beam passed through a differentially pumped gas cell filled with H_2. The pressure of the target gas was measured with a capacitance manometer, and was held constant with a feedback control valve to a precision of better than 1%.

L x rays of Cu were observed with a Si(Li) detector mounted perpendicular to the beam direction. The active area of the detector crystal was 30 mm^2, and the thickness of the beryllium window at the entrance of the detector was 0.008 mm. The distance between the ion beam and the detector crystal was about 20 mm, and the effective target length was also about 20 mm.

Following the collision cell a magnet was used to separate the different projectile charge states emerging from the collision region. The main beam component was collected in a Faraday cup and measured using a Keithley electrometer and current integrator, while projectiles with emerging charge states $q-1$ and $q+1$ (single capture and loss, respectively) were detected using silicon solid-state surface barrier detectors with 100% detection efficiency. Standard fast coincidence electronics were used to record copper L x rays associated with charge-changed projectiles. Using a VAX computer system and the CHAOS data acquisition software package [18], data were stored in event mode. All yields of interest were measured as a function of target gas pressure to obtain the desired cross sections, and to ensure that single-collision conditions prevailed.

The efficiency of the x-ray detector and the solid angle subtended by the detector were calculated from the detector properties and the geometry of the experimental arrangement. The model used for the detector was similar to that presented by Pajek *et al.* [19]. Details of the efficiency calibration method used can be found in Ref. [20]. In a separate measurement of K-shell x rays for 3-MeV H^++Ne and Ar collisions, for which the emitted K x rays have energies slightly less and more, respectively than the Cu L x rays of interest here, we obtained relative yields which were normalized to the known absolute cross sections [21–23] for these collision system. These normalization constants were also used as inputs to the model calculation. Because the x-ray detector efficiency varies rapidly in the range of Cu L x rays, a precise *in situ* energy scale calibration was performed using Ne, Al (from slit scattering), and Ar $K\alpha$ x rays measured during the efficiency calibration.

IV. RESULTS AND DISCUSSION

A typical copper L x-ray spectrum for Na-like Cu^{18+} is shown in Fig. 3. The projectile energy in this case was 65 MeV. The prominent maximum in the spectrum, centered at about 1100 eV, is due to x rays resulting from L-M transitions following L-shell excitation to $n\geq 3$. The higher-energy x rays near 1400 eV in the spectrum probably originate in the direct decay of the $n\geq 4$ excited states to the $n=2$ state.

Figure 4 shows the principal result of this work, namely, the measured cross sections for L x-ray emission associated with single-electron capture in $Cu^{18+}+H_2$ collisions, and the corresponding calculated RTEX cross sections. The energy

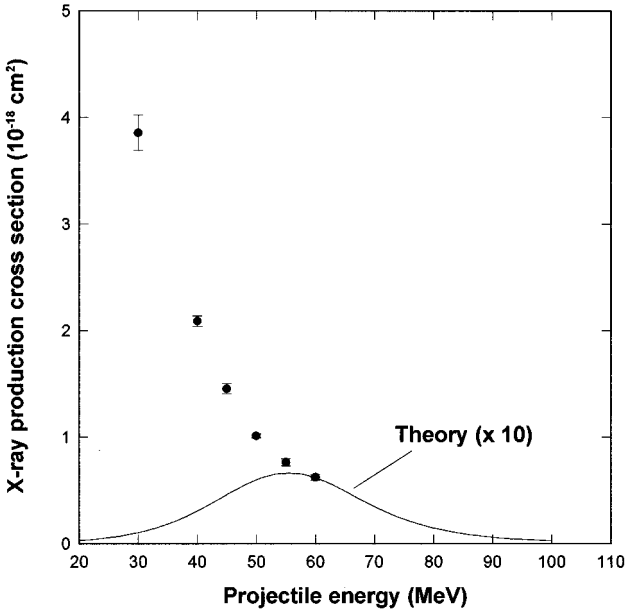

FIG. 5. X-ray production cross sections for single-electron capture coincident with L x-ray emission as a function of projectile energy in $Cu^{19+}+H_2$ collisions. The solid points are the present experimental data and the smooth curve shows the calculated RTEX cross sections multiplied by 10.

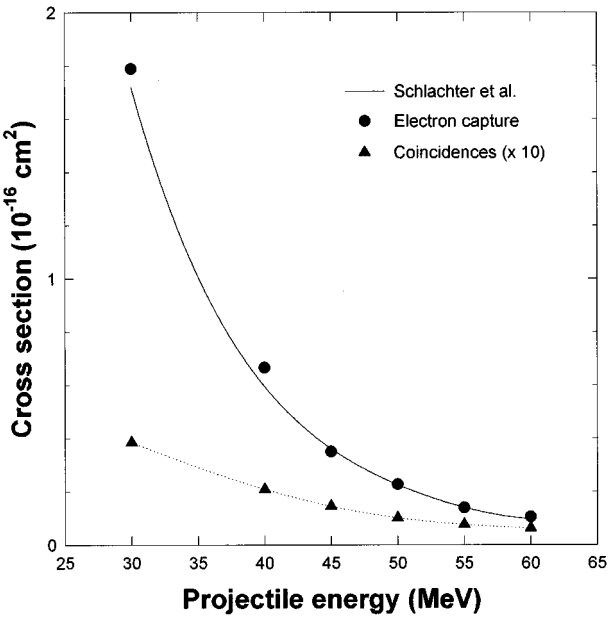

FIG. 6. Measured cross sections for total single electron capture and single-electron capture coincident with Lx-ray emission as a function of projectile energy in $Cu^{19+}H_2$ collisions. Symbols: ●, total single electron capture cross sections; △, coincidence cross sections multiplied by 10. The solid line is the empirical scaling law for total single electron capture of Schlachter *et al.* [27]. The dashed line is drawn to guide the eye.

plotted is that of the projectile in the laboratory frame. The measured cross sections for L x-ray production coincident with single capture are only ~15% of the total L x-ray production cross sections (not shown) at the position of the resonant maximum, in contrast with previous measurements for La^{40+} and Nb^{31+} [11,12], where this fraction is more nearly 50%.

The maximum near 60 MeV in Fig. 4 is due to the resonant production of $L^{-1}MM$ states, and the maximum near 100 MeV is due to the resonant production of $L^{-1}Mn$ ($n \geqslant 4$) states. These are the first experimental L-shell RTEX measurements involving $L^{-1}MM$ resonant states which have been compared with theoretical calculations (the earlier Nb^{q+} data [11,12] involved $L^{-1}MN$ resonant states only). We could not obtain data above 72 MeV due to the limitations of the accelerator and the 90° analyzing magnet. The error bars on the experimental data points are statistical uncertainties only. The overall experimental uncertainty is estimated to be about 30% due mainly to the uncertainty in the x-ray detector efficiency. Because the detector calibration method relies on previously determined Ne Auger electron production cross sections [21], the fluorescence yield for Ne [22], and the Ar K x-ray production cross section [23], all the uncertainties from these data are propagated in the present absolute cross-section values.

The theoretically predicted energy at which the $L^{-1}MM$ states are resonantly produced is in good agreement with the experimental value (~65 MeV). However, the theoretical values are about 60% lower than the experimental data. A partial explanation for this discrepancy could be the omission of angular effects in the x-ray emission during the RTEX process [24]. However, an estimate of the magnitude of these angular effects on decay of the $L^{-1}MM$ resonant states at 90° observation angle (as in the experiment) gives a theoretical value greater by only ~15%.

Figure 5 shows the measured cross sections for single-electron capture coincident with L x-ray emission as a function of the projectile energy for $Cu^{19+}+H_2$ collisions. Also shown are the calculated RTEX cross sections for this same collision system. It is seen that the data show no resonant behavior, and the magnitude of the measured cross section values is about one order of magnitude larger than the theoretical predictions. The monotonic decreasing behavior of the measured cross sections with increasing projectile energy is typical of electron capture cross sections.

The reason for the failure to see resonant behavior due to L-shell RTEX in $Cu^{19+}+H_2$ collisions is most likely due to the following. In the charge-stripping process to produce the Ne-like Cu^{19+} beam, an unknown fraction of metastable ions with the configuration $2p^5 3s\ ^3P_2$ is produced in the incident beam. Hence, these metastable ne-like ions have an initial vacancy in the L shell. The spontaneous decay of the $2p^5 3s\ ^3P_2$ metastable state of Ne-like Cu ions produced by post-stripping in a carbon foil was observed by Schiebel and Doyle [25]. For these Ne-like metastable ions, a target electron may be captured directly into a shell with $n \geqslant 3$ in a nonresonant process mediated by the projectile nucleus—target electron interaction. Subsequently, an L x ray can be emitted during the deexcitation of this intermediate excited state, thereby filling the L-shell vacancy. This process has the same signature as the RTEX process (single-electron capture coincident with L x-ray emission), yet occurs under nonresonant conditions and, hence, should exhibit the behavior of electron-capture cross sections. For comparison, in Fig. 6 we show the total single capture cross sections for $Cu^{19+}+H_2$ measured in this work, along with the cross sec-

tions for L x-ray emission accompanied by single-electron capture from Fig. 5. The general behavior of the two sets of data are seen to be similar. Also shown in the figure is the empirical scaling calculation for total single capture of Schlachter *et al.* [26] for $Cu^{19+}+H_2$ which is seen to be in good agreement with the data.

V. CONCLUSIONS

We have measured the energy dependence of L x-ray production associated with single-electron capture for Na-like Cu^{18+} and Ne-like Cu^{19+} ions colliding with H_2. Measurement of the energy dependence of these cross sections can provide a clear signature of the existence of L-shell RTEX, and give absolute values for the magnitude of the process. For $Cu^{18+}+H_2$ the maximum corresponding to the resonant production of $L^{-1}MM$ states occurs at the theoretically predicted value. An improved theoretical calculation of the cross sections removes the previous overestimation by a factor of 2 of the DR and RTEX experimental cross sections for Fe^{15+} and Nb^{30+}, respectively. However, this calculation now underestimates the present experimental cross sections by about 60% (~45% if one takes into account angular effects). Due to the uncertainties in the accuracy of the x-ray detector efficiency calibration, the 30% systematic error quoted in the experimental data may be optimistic, however; hence this could explain most of the remaining discrepancy between theory and experiment.

The cross sections for L x-ray production coincident with single-electron capture for Ne-like Cu^{19+}projectiles exhibit no resonant behavior, while RTEX theory predicts a resonant maximum to occur at ~55 MeV. The data instead exhibit a behavior typical of electron-capture cross sections. The reason for this behavior is likely due to a considerable metastable component in the incident projectile beam which can give rise to nonresonant capture followed by subsequent L x-ray emission.

Based on the results presented here, and considering earlier RTEX and DR measurements involving L-shell excitation, it appears that more work needs to be done to resolve the remaining discrepancies between theory and experiment for L-shell RTEX and possibly DR as well.

ACKNOWLEDGMENT

This work was supported in part by the U.S. Department of Energy, Office of Basic Energy Sciences, Division of Chemical Sciences.

[1] J. H. McGuire, Phys. Rev. A **36**, 1114 (1987).
[2] J. A. Tanis, S. M. Shafroth, J. E. Willis, M. Clark, J. Swenson, E. N. Strait, and J. R. Mowat, Phys. Rev. Lett. **47**, 828 (1981).
[3] J. A. Tanis, E. M. Bernstein, W. G. Graham, M. Clark, S. M. Shafroth, B. M. Johnson, K. Jones, and M. Meron, Phys. Rev. Lett. **49**, 1325 (1982).
[4] See, for example, Y. Hahn and K. J. LaGattuta, Phys. Rep. **166**, 196 (1988).
[5] H. S. W. Massey and D. R. Bates, Rep. Prog. Phys. **9**, 62 (1942).
[6] D. Brandt, Phys. Rev. A **27**, 1314 (1983).
[7] J. A. Tanis, in *Recombination of Atomic Ions*, edited by W. G. Graham, W. Fritsch, Y. Hahn, and J. A. Tanis (Plenum, New York, 1992), p. 241.
[8] T. Zouros, in *Recombination of Atomic Ions*, edited by W. G. Graham, W. Fritsch, Y. Hahn, and J. A. Tanis (Plenum, New York, 1992), p. 271.
[9] J. S. Lee, J. Chem. Phys. **66**, 4906 (1977).
[10] F. Briggs, L. B. Mendelsohn, and J. B. Mann, At. Data. Nucl. Data Tables **16**, 21 (1975).
[11] E. M. Bernstein, M. W. Clark, J. A. Tanis, K. H. Berkner, R. J. McDonald, A. S. Schlachter, J. W. Stearns, W. G. Graham, R. H. McFarland, T. J. Morgan, J. R. Mowat, D. W. Mueller, and M. P. Stockli, J. Phys. B **20**, L505 (1987).
[12] E. M. Bernstein, N. W. Clark, J. A. Tanis, W. T. Woodland, K. H. Berkner, A. S. Schlachter, J. W. Stearns, R. D. DuBois, W. G. Graham, T. J. Morgan, D. W. Mueller, and M. P. Stockli, Phys. Rev. A **40**, 4085 (1989).
[13] Y. Hahn, J. N. Gau, G. Omar, and M. P. Dube, Phys. Rev. A **36**, 576 (1987).
[14] N. R. Badnell, Phys. Rev. A **42**, 204 (1990).
[15] J. Linkemann, J. Kenntner, A. Müller, A. Wolf, D. Hads, D. Schwalm, W. Spies, O. Uwira, A. Frank, A. Liedtke, G. Hofmann, E. Salzborn, N. R. Badnell, and M. S. Pindzola, Nucl. Instrum. Methods Phys. Res. B **98**, 154 (1995).
[16] T. W. Gorczyca and N. R. Badnell, Phys. Rev. A **54**, 4113 (1996).
[17] N. R. Badnell, J. Phys. B **19**, 3827 (1986).
[18] W. Rathbun, Lawrence Berkeley Natl. Laboratory, Report No. LBL-29734, 1991 (unpublished).
[19] M. Pajek, A. P. Kobzev, R. Sandrik, R. A. Ilkhamov, and S. H. Khusmurodov, Nucl. Instrum. Methods Phys. Res. B **42**, 346 (1989).
[20] J. A. Wroblewski, Master's Thesis, Western Michigan University, 1996 (unpublished).
[21] C. W. Woods, R. L. Kauffman, K. A. Jamison, N. Stolterfoht, and P. Richard, Phys. Rev. A **13**, 1358 (1976).
[22] J. H. Hubbel, P. N. Trehan, N. Singh, B. Chand, D. Mehta, M. L. Garg, R. R. Garg, S. Sing, and S. Puri, J. Phys. Chem. Ref. Data **23**, 339 (1994), and references therein.
[23] L. M. Winters, J. R. Macdonald, M. D. Brown, L. D. Ellsworth, and T. Chiao, Phys. Rev. A **7**, 1276 (1973).
[24] C. P. Bhalla, in *Recombination of Atomic Ions*, edited by W. G. Graham, W. Fritsch, Y. Hahn, and J. A. Tanis (Plenum, New York, 1992), p. 87.
[25] U. Schiebel and B. L. Doyle, Z. Phys. A **285**, 241 (1978).
[26] A. S. Schlachter, J. W. Stearns, W. G. Graham, K. H. Berkner, and J. A. Tanis, Phys. Rev. A **27**, 3372 (1983).